

# PHOTOMETRIC CALIBRATION OF MOROI ALL-SKY CAMERAS: INTRODUCTION AND FIRST RESULTS

SIMON ANGHEL<sup>1,2</sup>, MIREL BIRLAN<sup>3,1</sup>, DAN-ALIN NEDELICU<sup>1,3</sup>, IOANA BOACA<sup>1</sup>

<sup>1</sup> *Astronomical Institute of Romanian Academy  
Str. Cutitul de Argint 5, 040557 Bucharest, Romania  
Email: simon.anghel@aira.astro.ro*

<sup>2</sup> *Faculty of Physics, University of Bucharest  
405-Atomistilor, 077125 Magurele, Ilfov, Romania*

<sup>3</sup> *Institut de Mécanique Céleste et de Calculs des Éphémérides, CNRS UMR 8028,  
Observatoire de Paris, PSL Research University,  
77 Av. Denfert-Rochereau, 75014 Paris Cedex, France*

*Abstract.* Latest advances in charged coupled devices (CCD) allowed the implementation of dense mesh fireball networks. Along with meteor studies, long term analysis of all-sky sequences of calibration captures can provide us with the number of nights we can use for astronomical observations, the number of photometric nights, how the atmospheric extinction changes around the sky or throughout the year. For this study we performed a systematic analysis for two stations of Meteorites Orbits Reconstruction by Optical Imaging (MOROI) network. We implemented a method to characterize the photometric nights, and we established an integral extinction of 0.56 magnitudes/air mass for Feleac, and 0.48 magnitudes/air mass for Berthelot. These yearly coefficients will be used to calibrate the photometry for meteor events.

*Key words:* All-sky – Photometry – Atmospheric Extinction – Bouguer.

## 1. INTRODUCTION

The long endeavor of bridging the gaps between asteroids, meteoroids and meteorites has led to a necessity for fireball networks. These networks concentrate mostly on meteor studies and the recovery of meteoritic material (Devillepoix *et al.*, 2018; Colas *et al.*, 2018). The data accumulated within a fireball network can be later used to either connect the meteors to parent bodies (Jenniskens *et al.*, 2011; Jopek and Williams, 2013; Rudawska *et al.*, 2016; Dumitru *et al.*, 2017), or model various aspects of meteoroid interactions with the atmosphere. Popova *et al.* (2011) assembled 13 cases of meteorite falls with accurate tracking records, which indicate the validity of mass estimation via photometry. Gritsevich and Koschny (2011) proposed a method to combine the photometric measurements of meteors with dynamical data to constrain the mass estimations for objects entering the Earth's atmosphere. However, these measurements need to be calibrated for external factors, including atmospheric extinction, cloud coverage, the optical limitations of the setup, and digital



Fig. 1 – The MOROI network map: Feleac (1), Berthelot (2), Mărișel (3), Păulești (4), Timișoara (5), București (6), Dej (7), Galați (8), Bârlad (9), Bocșa (10), Mădârjac (11).

characteristics of the CCD. For a fireball network, these calibrations can be accomplished with the aid of long term data collected at regular intervals, and to the extent of all-sky cameras, these regular captures are also valuable for astroclimate characterizations. Such measurements are already a requisite to characterize observatory locations (Taylor, Jansen, and Windhorst, 2004; Hogg *et al.*, 2001).

For this study we conducted an analysis on all-sky data, for the first two installed cameras (*i.e.* Feleac and Berthelot) within the MOROI network (Figure 1). We compared the atmospheric extinction and the number of clear nights, during a period of days, months and a year. We also implemented a quadrant division in the extinction analysis to discover possible dichotomies between different directions along the azimuth.

## 2. EQUIPMENT

Measurements of night sky brightness, the number of clear nights, or photometric stability have been done before, and some of these studies rely on specialized cameras and filter setup in an effort to characterize the sky-quality for a particular observatory and can measure the atmospheric extinction for multiple pass bands (Aceituno *et al.*, 2011). Though these designated instruments are highly desirable, a systematic analysis can be obtained only with a dense mesh of cameras covering a certain area, and in our case, we rely on the already established MOROI fireball network.

The MOROI project started in 2017 (Nedelcu *et al.*, 2018), with the first Fireball Recovery and InterPlanetary Observation Network (FRIPON) camera installed in Bucharest, and currently consists of 11 systems of cameras deployed over the territory of Romania. The plan is to extend the number of cameras to 20, aiming for an interval of less than 100 kilometers between stations, in order to triangulate meteoric events.



Fig. 2 – FRIPON cameras on the roof of Astronomical Institute of the Romanian Academy in Bucharest (left) and Observatoire de Paris, Paris (right).

Analogous to FRIPON (Colas *et al.*, 2014) and PRISMA (Gardiol, Cellino, and Di Martino, 2016), the setup design is quite simple. A node has two main parts (i.e. the camera and the computer) connected via Ethernet. The camera unit (Figure 2) includes a DMK 23G445 camera, which is based on the  $5 \times 4$  mm Sony chip ICX445 (1280  $\times$  960 active pixels, 12 bit dynamical range). The exposure time ranges from 30s, which allows for astrometrical calibration frames, down to  $10\mu\text{s}$  for daytime observations. GigE-Vision protocol was chosen due to the versatility of power over Ethernet (PoE) as it allows cable (RJ45) up to 100m length. The data are stored locally as each node hosts an i3 Intel NUC with 1 TB HDD. This will cover all the necessary data storage for 3 years of operation. Some of our stations enter the third year, therefore, we already backed-up most of the data on the central node in Bucharest.

A bad lens can corrupt large areas on CCD, therefore, lens quality is critical for very bright fireballs. Although fish-eye lenses by definition produce a heavy

radial distortion, Focusave 1.25mm F/2.0 aperture presented the optimal choice, for its optical quality, ensuring a sampling of the whole sky, with a field of view of  $185^\circ$  (Figure 3). The camera housing has passive cooling, and is designed to withstand severe weather conditions (Colas *et al.*, 2014).

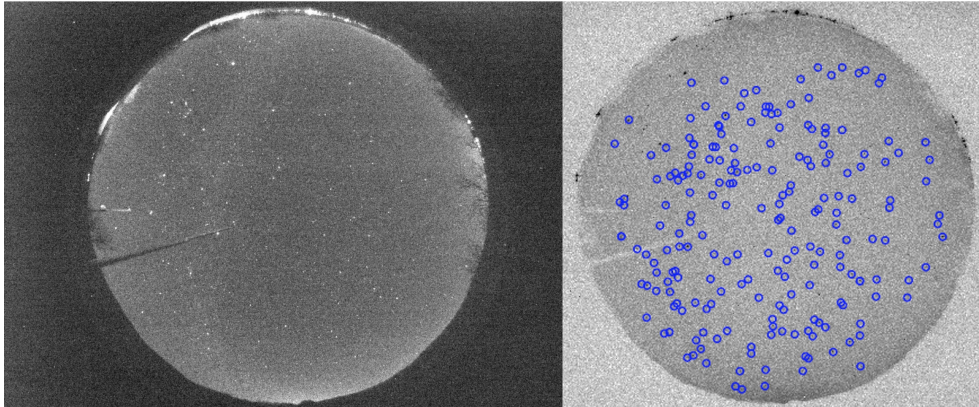


Fig. 3 – Left: example of *capture* from Berthelot station acquired on 5 March 2019, 20:27:55 UT. Right: the same *capture* and after the matching sequence. The blue circles enclose detected sources associated with catalogue stars ( $N_\star = 205$ ). For this night, the  $N_\star \max$  is 229.

### 3. DATA REDUCTION

Each station uses *FreeTure* software (Audureau *et al.*, 2014) for both meteor detection and image acquisition. The software is fully automated and can be adjusted for nighttime or daytime observations. In order to calibrate the events and to characterize the sky quality, the software collects a 5 seconds ( $20\mu\text{s}$  during daytime) long exposure *capture* every 15 minutes, which is stored in FITS format. In the image header we can find the camera settings along with information necessary for the star matching sequence.

To obtain the catalog designations of stars in the image we need to match the calculated star positions, with light sources detected in *captures*. For the source detection we use the *DAOStarFinder* routine (*Photutils*) based upon *DAOFIND* (Stetson, 1987) algorithm. The orientation of the *capture* is with positive  $x$  axis towards E and  $y$  axis towards S. The routine searches for local density maxima with peak amplitude over a predefined threshold and returns the image coordinates for all the possible light sources ( $x,y$  observed). Next, we construct a table of calculated positions of stars (brighter than magnitude 6) using the date and time of the image along with the geographic coordinates of the station. These help assemble a grid with the

altitude and the azimuth of the stars that should be on the sky, and apply a radial distortion function that we obtain empirically (at the time of station setup) to obtain the coordinates on the image ( $x,y$  calculated). Finally, to associate the known stars, we keep only observed sources within two pixels from calculated stars (Figure 3). For these stars we build a table of attributes combining the elements obtained from *DAOStarfinder* (observed coordinates, instrumental magnitude, *peak*, *flux*, etc) with the results of the associated star (calculated coordinates, *Bayer ID*, *catalog V magnitude*, altitude, azimuth, etc) in order to use it for further analysis.

Within image treatment routines, a proper frame correction is required in order to obtain qualitative data. For all-sky cameras installed in remote locations, obtaining such corrections (dark, flat, bias) proves to be troublesome. Unlike the usual astronomical imaging, the all-sky *captures* are grabbed continuously on an automated scheduler (every 15 minutes) to maximize the time allocated for meteor detection. To filter the data for our two stations and obtain a final group set of *captures*, we applied a threshold of the minimum number of stars for each station and the star magnitude limit. We chose this method to minimize the errors, while keeping a statistical significant sample for analysis. This may change for images with lower SNR stars (within cities), hence we will consider an image post processing routine (Jeanne *et al.*, 2019; Barghini *et al.*, 2019).

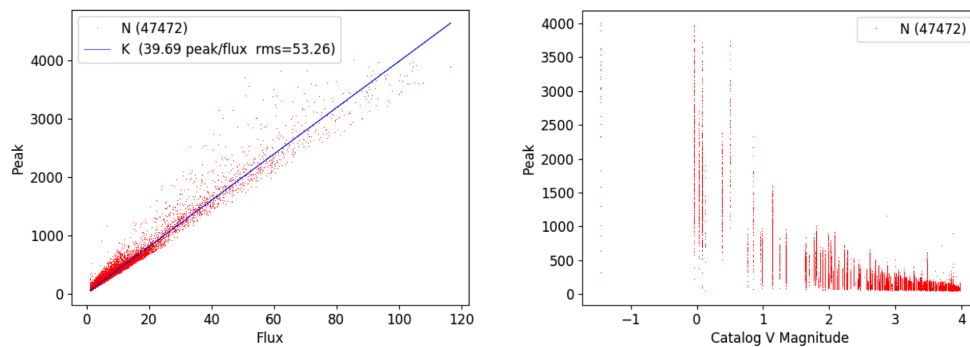


Fig. 4 – The *peak* values of stars during photometric nights of March 2019 on Berthelot station, as a function of *flux* and the star's *Catalog V Magnitude* (visual filter band). The latter graph illustrates the distribution of peak values a star can obtain during the month, mostly due to atmospheric extinction.

For this analysis we discarded bright sources that reached the CCD saturation level, and due to a higher noise towards dimmer objects, we kept only the stars brighter than magnitude 4.

During the exposure needed for the *capture* (5s) some of the brightest stars can reach the CCD saturation level, which for our cameras is 4096. The *peak* is the maximum pixel value in ADUs of the object (i.e., star) after the sky median subtraction and the sum of pixel values in the convolved image is the *flux*. Thus, an increase in *peak* for detected stars should be closely linked with an increase in *flux*

(Figure 4). From this we can then obtain the instrumental magnitude ( $m_{inst}$ ):

$$m_{inst} = -2.5 \log_{10} (Flux) \quad (1)$$

On photometric nights the ( $m_{inst}$ ) can be significantly affected by the mass of air. If we take the *airmass* at the zenith as a unit, the air mass  $m$  in any direction is a function of zenith distance  $z$ :

$$airmass = \frac{1}{\cos z} \quad (2)$$

To obtain the coefficient as a function of air mass we first have to subtract the  $m_{inst}$  from the tabulated magnitude ( $m_{cat}$ ) for each matched star:

$$m_{calib} = m_{cat} - m_{inst} \quad (3)$$

We then plot  $m_{calib}$  as a function of air mass and the linear regression of the values is the Bouguer extinction law (Figure 5). Though we can not separate the atmospheric extinction from the intrinsic vignetting of the optical system, the consequent objective of this procedure is to obtain a calibration coefficient ( $K$ ) for meteor light curves.

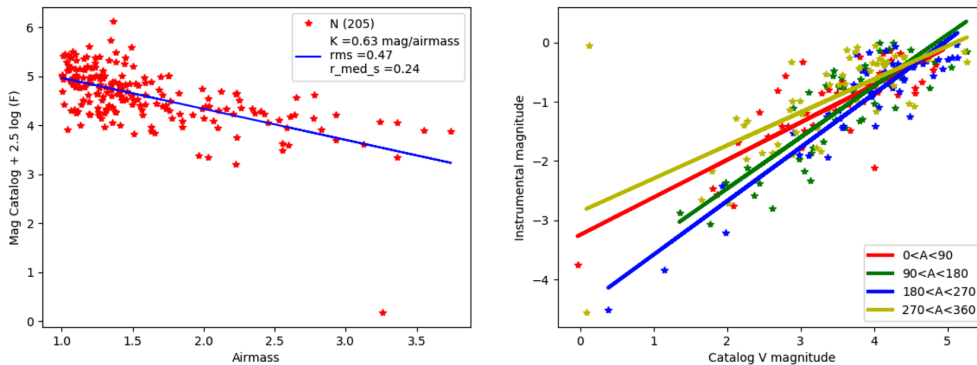


Fig. 5 – Left: Example of extinction line for the matched stars of 5 March 2019, 20:27:55 UT at Berthelot.  $N$  is the number of stars,  $K$  is the extinction coefficient,  $rms$  and  $r_{med_s}$  are the root mean square and the root median square of the regression line. Right: Photometric calibration for the same set of stars.

To observe dichotomies along the azimuth we divided the sky into four quadrants (Figure 6), and obtained an extinction coefficient for each quadrant.

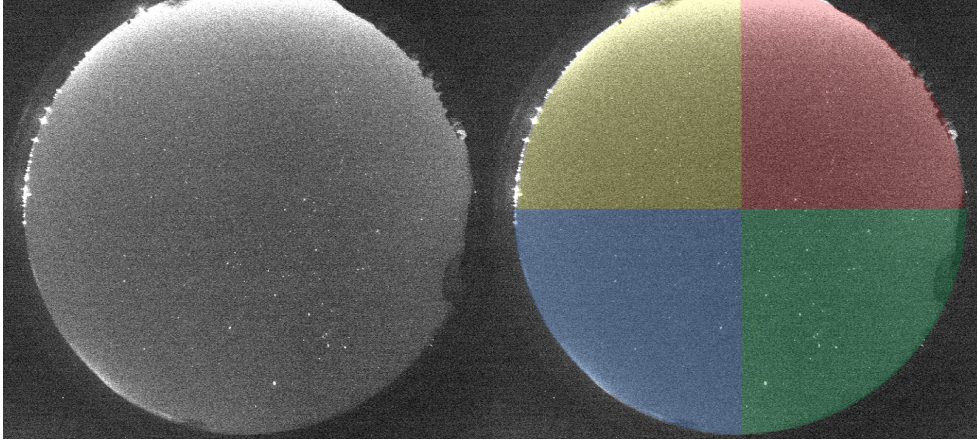


Fig. 6 – Left: Example of *capture* from Feleac station acquired on 5 March 2019, at 18:37:38 UT. Right: A color coded division into quadrants along the azimuth for the same *capture*. The bright horizon in the upper part of the image light pollution over the city of Cluj-Napoca.

#### 4. APPLICATION FOR TWO STATIONS

To obtain the maximum number of stars for Feleac and Berthelot (Figure 7) we counted the number of associated stars on all the *captures* collected during a year (30.000 images) and plotted the best image of the day for each month. For Berthelot, the number of detections increased considerably after mid-November 2018, when we moved the camera to a darker site. Though, during the winter nights, star detections are sparse on both stations on account of clouds, but also due to rime or dew build-up onto the camera dome. A major player is the full Moon, as the sky background becomes brighter, and the majority of stars fall below the detection threshold.

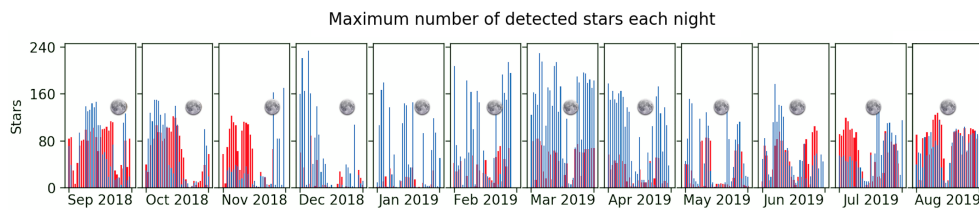


Fig. 7 – Histogram for the matched stars on the best *capture* for every night of the year for Feleac (red set) and Berthelot (blue set). The day with full Moon phase is displayed for each month.

For the full year raw data, we applied a threshold to obtain a subset of photometric images for the extinction analysis. We kept only the *captures* with more than 40 stars for Feleac. For Berthelot we selected a higher threshold (*i.e.*, *captures* with

more 100 stars). This threshold was introduced to reduce the sources of error, while still keeping a statistical significant sample for analysis.

The high variability of the final data set is caused by circumstances that reduce or amplify the light of stars (e.g. hot pixels, dust spots, reflections due to moon or other powerful lights).

The division along the azimuth can help on single *captures* when the sky is partly clouded, and a meteor is detected within the clear quadrant. However, when we track the behaviour of long term data, we can observe a clear azimuth dichotomy in Feleac (red and yellow lines in Figures 8 and 9), due to the effect of light pollution.

For Berthelot, a higher extinction (15%) is observed in the third quadrant, yet there is no clear source for the dichotomy.

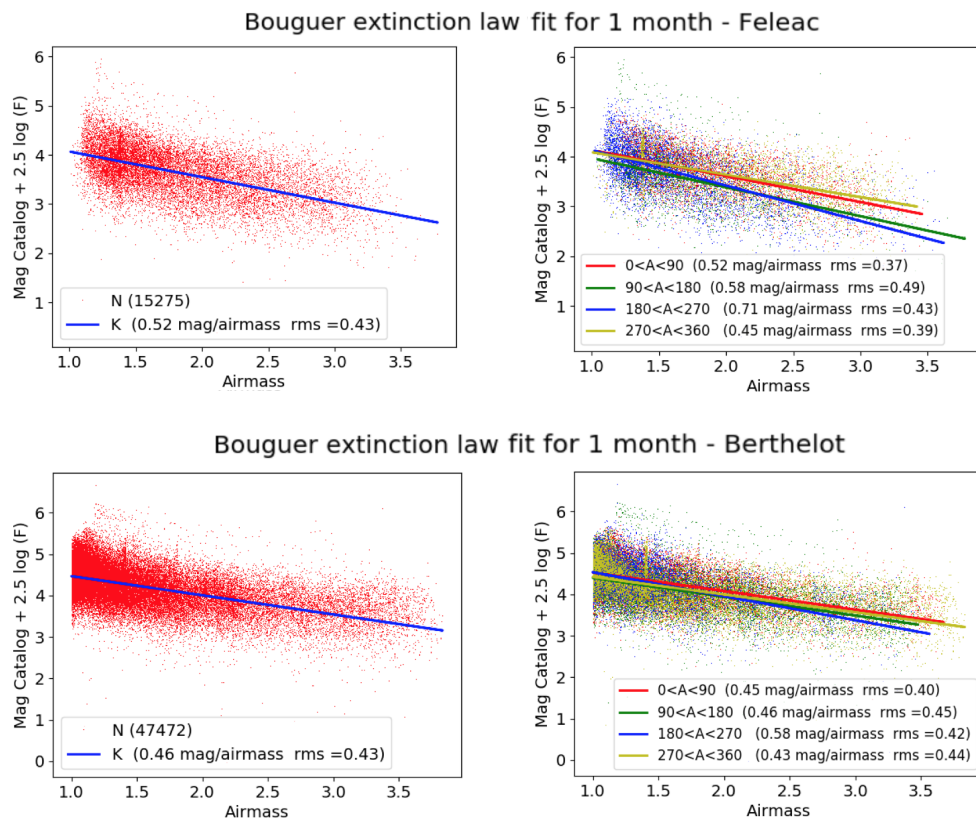


Fig. 8 – Distribution of calibrated stars as a function of air mass for Feleac and Berthelot.

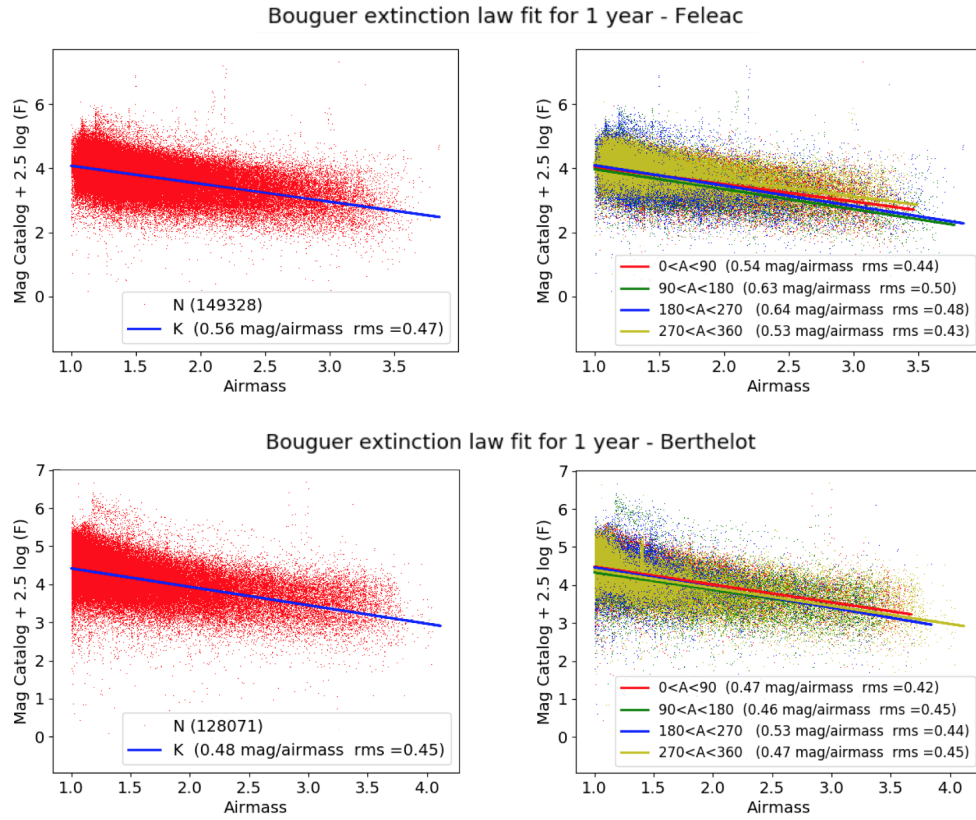


Fig. 9 – Distribution of calibrated stars as a function of air mass for Feleac and Berthelot.

## 5. SUMMARY AND CONCLUSION

We performed a study on all-sky photometry for two of MOROI stations, Berthelot and Feleac over the course of one year. This period translates into more than 30,000 images analyzed by our routine. Our algorithm can identify stars up to 130 stars on Feleac and 230 stars on Berthelot having magnitude 6 as the upper limit. For the photometric images (during 80 nights/year) we obtained an integral extinction of 0.56 magnitudes/air mass for Feleac and 0.48 magnitudes/air mass for Berthelot. This was obtained for a group set of *captures* selected by a threshold for the minimum number of detected stars, and the maximum magnitude. This ameliorated the uncertainty in the extinction by 50% compared to raw data. A division into months or seasons for the extinction coefficient is not yet feasible due to a disparity of associated stars during long cloudy periods. This will be revisited when we gather multiple years of data.

The number of detectable stars is a robust method to filter out the erroneous

detections, though fairly simplistic proxy to obtain the mean number of nights that can be used for astronomical observations. Aside from the atmospheric sources of error (*i.e.*, cloud coverage, cloud type, atmospheric aerosols), there are effects that will cause a high variability in the extinction analysis by reducing the light of associated stars. The camera domes need to be inspected regularly, especially during the winter or summer, as snow or dust build-up will impede the collection of data. The domes can also get damaged due to hail or scratched by birds (Figure 2) and will eventually require replacement. Furthermore, there are other systematic sources of error that insert false stars, or effects that amplify the light of stars. These include the hot pixels and reflections into the dome produced by powerful light sources as a result of human activity, or the Moon. On the other hand, during the nights around a full Moon, the sky background becomes brighter, and the majority of stars fall below the detection threshold. This phenomenon also occurs in large cities, or in areas near a city, and can be observed in the first and last quadrant on Feleac data (Figure 8 and 9). The light pollution from the city of Cluj-Napoca further charge the pixels in the Gaussian kernel for stars (*i.e.*, the stars will appear brighter) north of Feleac station (Figure 6).

A robust characterization of light pollution, the number of photometric nights, or nights we can use for observations becomes important for mobile platforms that can be assembled *ad-hoc* on remote locations (Birlan *et al.*, 2019). Moreover, a live sky coverage estimator is necessary for surveys using robotic telescopes that can update the observations schedule in real time.

These results along with the extinction obtained from the rest of the stations will be further used to calibrate the magnitudes of meteors already in MOROI database.

*Acknowledgements.* This work was supported by a grant of the Romanian Ministry of Research and Innovation, CCCDI - UEFISCDI, project number PN-III-P3-3.1-PM-RO-FR-2019-0075 / 5BM/2019, within PNCDI III.

## REFERENCES

- Aceituno, J., Sánchez, S., Aceituno, F.J., Galadí-Enríquez, D., Negro, J.J., Soriguer, R.C., Gomez, G.S.: 2011, An all-sky transmission monitor: *Astron. Publications of the Astronomical Society of the Pacific* **123**(907), 1076.
- Audureau, Y., Marmo, C., Bouley, S., Kwon, M.K., Colas, F., Vaubailon, J., Birlan, M., Zanda, B., Vernazza, P., Caminade, S., et al.: 2014, Freeture: A free software to capture meteors for fripon. In: *Proceedings of the International Meteor Conference, Giron, France, 18-21 September 2014*, 39–41.
- Barghini, D., Gardiol, D., Carbognani, A., Mancuso, S.: 2019, Astrometric calibration for all-sky cameras revisited. *Astronomy & Astrophysics* **626**, A105.
- Birlan, M., Sonka, A., Nedelcu, D.A., Balan, M., Anghel, S., Georgescu, T., et al.: 2019, Telescope

- calibration for mobile platforms: First results. *Romanian Astronomical Journal* **29**(1), 23–33.
- Colas, F., Zanda, B., Bouley, S., Vaubaillon, J., Vernazza, P., Gattacceca, J., Marmo, C., Audureau, Y., Kwon, M.K., Maquet, L., et al.: 2014, The fripon and vigie-ciel networks. In: *Proceedings of the 2014 International Meteor Conference, Giron, France*, 18–21.
- Colas, F., Baillié, K., Bouley, S., Zanda, B., Vaubaillon, J., Jeanne, S., Egal, A., Vernazza, P., Gattacceca, J., Birlan, M., et al.: 2018, Fripon and impact projects to pinpoint interplanetary matter in the centimetre-hundred meter range. In: *European Planetary Science Congress* **12**.
- Devillepoix, H.A., Bland, P.A., Sansom, E.K., Towner, M.C., Cupák, M., Howie, R.M., Hartig, B.A., Jansen-Sturgeon, T., Cox, M.A.: 2018, Observation of metre-scale impactors by the desert fireball network. *Monthly Notices of the Royal Astronomical Society* **483**(4), 5166–5178.
- Dumitru, B., Birlan, M., Popescu, M., Nedelcu, D.: 2017, Association between meteor showers and asteroids using multivariate criteria. *Astronomy & Astrophysics* **607**, A5.
- Gardioli, D., Cellino, A., Di Martino, M.: 2016, Prisma, italian network for meteors and atmospheric studies. In: *International Meteor Conference Egmond, the Netherlands, 2-5 June 2016*, 76–79.
- Gritsevich, M., Koschny, D.: 2011, Constraining the luminous efficiency of meteors. *Icarus* **212**(2), 877–884.
- Hogg, D.W., Finkbeiner, D.P., Schlegel, D.J., Gunn, J.E.: 2001, A photometricity and extinction monitor at the apache point observatory. *The Astronomical Journal* **122**(4), 2129.
- Jeanne, S., Colas, F., Zanda, B., Birlan, M., Vaubaillon, J., Bouley, S., Vernazza, P., Jorda, L., Gattacceca, J., Rault, J., et al.: 2019, Calibration of fish-eye lens and error estimation on fireball trajectories: application to the fripon network. *Astronomy & Astrophysics* **627**, A78.
- Jenniskens, P., Gural, P., Dynneson, L., Grigsby, B., Newman, K., Borden, M., Koop, M., Holman, D.: 2011, Cams: Cameras for allsky meteor surveillance to establish minor meteor showers. *Icarus* **216**(1), 40–61.
- Jopek, T., Williams, I.: 2013, Stream and sporadic meteoroids associated with near-earth objects. *Monthly Notices of the Royal Astronomical Society* **430**(3), 2377–2389.
- Nedelcu, D.A., Birlan, M., Turcu, V., Boaca, I., Badescu, O., Gornea, A., Sonka, A.B., Blagoi, O., Danescu, C., Paraschiv, P.: 2018, Meteorites Orbits Reconstruction by Optical Imaging (MOROI) Network. *Romanian Astronomical Journal* **28**(1), 57–65.
- Popova, O., Borovička, J., Hartmann, W.K., Spurný, P., Edwin, G., Nemtchinov, I., Trigo-Rodríguez, J.M.: 2011, Very low strengths of interplanetary meteoroids and small asteroids. *Meteoritics & Planetary Science* **46**(10), 1525–1550.
- Rudawska, R., Tóth, J., Kalmančok, D., Zigo, P., Matlovič, P.: 2016, Meteor spectra from amos video system. *Planetary and Space Science* **123**, 25–32.
- Stetson, P.B.: 1987, Daophot: A computer program for crowded-field stellar photometry. *Publications of the Astronomical Society of the Pacific* **99**(613), 191.
- Taylor, V.A., Jansen, R.A., Windhorst, R.A.: 2004, Observing conditions at mount graham: Vatican advanced technology telescope ubvr sky surface brightness and seeing measurements from 1999 through 2003. *Publications of the Astronomical Society of the Pacific* **116**(822), 762.

*Received on 27 November 2019*